



Obrabotka metallov -

Metal Working and Material Science







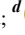







Journal homepage: http://journals.nstu.ru/obrabotka_metallov



Production of rods and sheets from TiNiHf alloy with high-temperature shape memory effect by longitudinal rolling and rotary forging methods

Roman Karelin^{a,*}, Viktor Komarov^b, Vladimir Cherkasov^c, Artem Osokin^d,
 Konstantin Sergienko^e, Vladimir Yusupov^f, Vladimir Andreev^g

A.A. Baykov Institute of Metallurgy and Materials Science of the Russian Academy of Sciences, 49 Leninsky Ave., Moscow, 119334, Russian Federation

^a  <https://orcid.org/0000-0002-4795-8668>,  rdkarelin@gmail.com; ^b  <https://orcid.org/0000-0003-4710-3739>,  vickomarov@gmail.com;
^c  <https://orcid.org/0000-0002-5450-3565>,  cherkasov.vv@misis.ru; ^d  <https://orcid.org/0009-0008-4945-3648>,  art.osokin1201@icloud.com;
^e  <https://orcid.org/0000-0003-4018-4599>,  shulf@yandex.ru; ^f  <https://orcid.org/0000-0002-0640-2217>,  vsyusupov@mail.ru;
^g  <https://orcid.org/0000-0003-3937-1952>,  andreev.icmateks@gmail.com

ARTICLE INFO

Article history:

Received: 07 July 2025

Revised: 28 July 2025

Accepted: 07 August 2025

Available online: 15 September 2025

Keywords:

Shape memory alloy

Rolling

Hardness

Rotary forging

Funding

The study was conducted with the financial support of the State Task of IMET RAS on 2025 year № 075-00319-25-00.

ABSTRACT

Introduction. *Ti-Ni* based shape memory alloys (*SMA*s) are functional materials that find widespread practical application in engineering and medicine. Functional properties of *Ti-Ni* based alloys are sensitive to the chemical composition. To develop alloys with specific properties, ternary *SMA*s are being actively developed. For example, *TiNiHf* ternary alloys are characterized by a high-temperature shape memory effect. Today, there is a demand for *SMA*s used in the production of functional elements with a response temperature of more than 120 °C. These alloys must also have sufficient ductility to obtain deformed semi-finished products for the subsequent manufacture of heat-sensitive functional elements. Also among the current issues of developing the practical application of *TiNiHf* alloys is the lack of technological schemes for obtaining semi-finished products from *TiNiHf SMA*s. **The purpose of this work** is study the feasibility of conducting deformation processing of the studied *TiNiHf* alloys with a high-temperature shape memory effect and to identify the relationships between phase composition and mechanical characteristics and the applied processing method. **In this work**, the possibility of producing sheets and rods from *TiNiHf* alloys with 5 and 10 at.% *Hf* and 50.0 at.% *Ni* by longitudinal rolling, caliber rolling, and rotary forging was investigated. **The research methods** were: X-ray analysis, differential scanning calorimetry, and measurement of *Vickers* hardness. **Results and discussion.** It was found that the *TiNiHf* alloy with 10 at.% *Hf* has insufficient ductility. From the alloy with 5 at.% *Hf*, blanks in the form of sheets and rods of various sizes were obtained by using longitudinal rolling and rotary forging processes. It was shown that hot deformation allows increasing the hardness of the studied *TiNiHf* alloy with 5 at.% *Hf* compared to the cast state, from 232 HV to 242–264 HV. Cold deformation leads to a significant increase in hardness values up to 362–394 HV. Characteristic temperatures of the forward and reverse martensitic transformation are quite stable. The obtained results indicate the potential of using longitudinal rolling and rotary forging to obtain semi-finished products of *TiNiHf* alloys with 5 at.% *Hf* and to improve the functional and mechanical properties of the alloy after smelting.

For citation: Karelin R.D., Komarov V.S., Cherkasov V.V., Osokin A.A., Sergienko K.V., Yusupov V.S., Andreev V.A. Production of rods and sheets from TiNiHf alloy with high-temperature shape memory effect by longitudinal rolling and rotary forging methods. *Obrabotka metallov (tekhnologiya, oborudovanie, instrumenty)* = *Metal Working and Material Science*, 2025, vol. 27, no. 3, pp. 37–49. DOI: 10.17212/1994-6309-2025-27.3-37-49. (In Russian).

Introduction

Shape memory alloys (*SMA*s) based on titanium nickelide are functional materials that receive widespread practical application in engineering and medicine due to their unique shape memory properties, high mechanical characteristics, corrosion resistance, and biocompatibility [1–7]. In order to regulate their

* Corresponding author

Karelin Roman D., Ph.D. (Engineering),
 A.A. Baykov Institute of Metallurgy and Materials Science
 of the Russian Academy of Sciences,
 49 Leninsky ave.,
 119334, Moscow, Russian Federation
Tel.: +7 916 590-42-76, **e-mail:** rdkarelin@gmail.com

functional behavior and obtain materials with special properties, the use of ternary titanium nickelide alloys containing *Cu*, *Fe*, *Co*, *Nb*, and *Hf* is being actively developed [8–11]. Among these alloys for high-temperature applications, alloys of the *TiNiHf* system should be highlighted [12–14]. Most scientific research in this field focuses on alloys with 20 at.% *Hf* and 50.3 at.% *Ni*, which provide a temperature range of shape recovery (*TRSR*) of 200–350 °C [15–19]. The high *Hf* (20 at.%) and *Ni* (over 50 at.%) content is attributed to observations from previous studies, which suggest that *TiNiHf* alloys become brittle and difficult to deform when the combined concentration of *Ti* and *Hf* exceeds 49.8 at.%. Embrittlement is attributed to the precipitation of a significant amount of an embrittling (*Ti*, *Hf*)₂*Ni*-type phase [20]. To mitigate this, the nickel concentration is typically increased. However, if other elemental contents remain unchanged, the martensitic transformation temperature range will decrease accordingly. Therefore, a higher *Hf* concentration is required to achieve a high-temperature shape memory effect in these alloys. However, high *Hf* content significantly increases the cost, hindering their practical application. Moreover, the application of *TiNiHf* *SMA*s is also challenged by the limited control over martensitic transformation temperatures. Several industries currently require shape-memory alloys with a *TRSR* ranging from 120 to 200 °C, coupled with sufficient technological plasticity for the production of thermosensitive components. In addition, a significant challenge in expanding the practical applications of *TiNiHf* alloys lies in developing the technology for manufacturing semi-finished products of various grades, a task inextricably linked to the advancement of novel thermomechanical processing methods [21].

Earlier studies showed that rods with high mechanical properties and a shape recovery temperature of 155 °C after 2% bending could be obtained from the *Ti*_{49.0}*Ni*_{49.5}*Hf*_{1.5} alloy using rotary forging [22]. Reference [23] also demonstrated that a pulsed electric current could improve the technological plasticity of the *Ti*_{47.4}*Ni*_{47.6}*Hf*_{5.0} alloy during cold rolling.

Based on the preceding discussion, and as part of our effort to develop methods for creating semi-finished *TiNiHf* *SMA* products with lower *Hf* and *Ni* content, the first purpose of this study is to explore the application of thermomechanical treatments to *TiNiHf* alloys with 5 and 10 at.% *Hf* and 50 at.% *Ni*, using different deformation methods. The second purpose is to determine how the phase composition and mechanical characteristics of *TiNiHf* alloys change depending on the deformation method used.

This paper investigates the production of semi-finished sheets and rods using longitudinal rolling, caliber rolling, and rotary forging. The alloy's structure and mechanical properties were also analyzed using X-ray analysis, differential scanning calorimetry, and *Vickers* hardness testing. A significant result is the successful production of *Ti*_{45.0}*Ni*_{50.0}*Hf*_{5.0} alloy semi-finished products, including sheets (2.2 and 1.0 mm thick), a rectangular bars (6.9 × 8.5 mm), and a 5.1 mm diameter rods, all demonstrating high hardness and stable phase composition.

Methods

The study used two alloys with compositions *Ti*_{45.0}*Ni*_{50.0}*Hf*_{5.0} and *Ti*_{40.0}*Ni*_{50.0}*Hf*_{10.0}. The starting materials were 99.99% pure iodide titanium, 99.99% pure nickel (*H0* grade), and 2.5 mm diameter hafnium wire (*GFI-1* grade). *TiNiHf* ingots containing 5 and 10 at.% *Hf* were produced by vacuum electric arc melting, with eight remelting cycles, and cast into a water-cooled copper mold. Hot deformation was performed by longitudinal flat and bar rolling on a *DUO 300* two-roll rolling mill and by rotary forging at 850 °C. The bar rolling used a square-to-square pass schedule, with the square side changing as follows: 19→17→15→13→11→9→8→7→6 mm. Cold rolling was then performed on a *QUARTO110/300* four-roll rolling mill.

The martensitic transformation temperature range (*TRMT*) in the as-cast alloy was studied by differential scanning calorimetry (*DSC*) using a *Mettler Toledo DSC 3+* calorimeter with a heating and cooling rate of 10 °C/min from 0 to 200 °C.

The martensitic transformation temperature range (*TRMT*) was measured using differential scanning calorimetry (*DSC*) on a *Mettler Toledo DSC 3+* calorimeter, with a heating/cooling rate of 10 °C/min from 0 to 200 °C. The phase composition was analyzed by X-ray diffraction analysis (*XRD*) using a *DRON-3*

diffractometer with $CuK\alpha$ radiation at 2θ angles from 35 to 47° [18, 24]. *Vickers* hardness was measured at room temperature using a *LECOM 400-A* hardness tester under a 1 N load to determine mechanical properties.

Result and Discussion

Initial $TiNiHf$ SMA Ingots

Fig. 1 shows the general appearance of the ingots produced by electron beam melting. Table 1 presents the mass, dimensions, and chemical composition of the ingots.

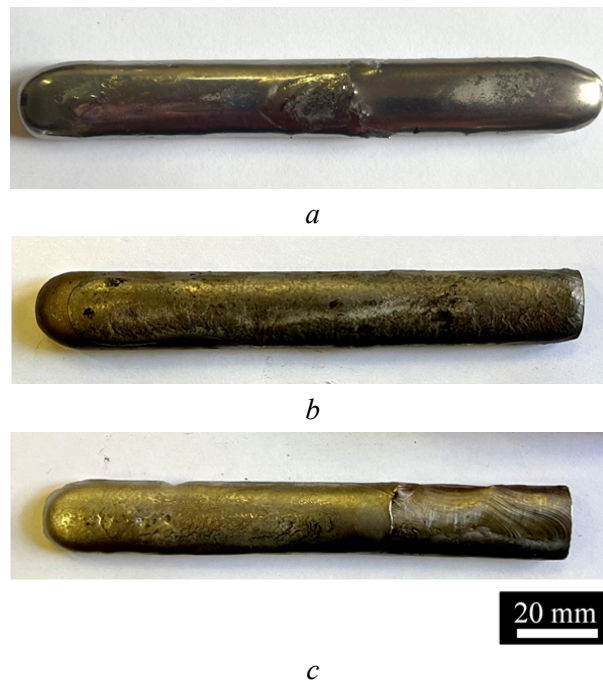


Fig. 1. Photographs of ingots 1 (a), 2 (b), and 3 (c) of $TiNiHf$ SMA after vacuum arc melting with 8-fold remelting

Table 1

Weight, dimensions and estimated composition of the $TiNiHf$ ingots

Ingot No.	Weight, g	Dimensions, ($h \times b \times L$) mm	Chemical composition					
			mass %			at. %		
			<i>Ti</i>	<i>Ni</i>	<i>Hf</i>	<i>Ti</i>	<i>Ni</i>	<i>Hf</i>
1	148.84	$9.5 \times 18.1 \times 137.5$	28.87	44.23	26.90	40.0	50.0	10.0
2	150.15	$10.4 \times 18.5 \times 136.9$	36.03	49.06	14.92	45.0	50.0	5.00
3	149.12	$9.8 \times 17.8 \times 137.5$	28.87	44.23	26.90	40.0	50.0	10.0

After melting, the martensitic transformation temperature range (*TRMT*) of the ingots was analyzed using differential scanning calorimetry (*DSC*). Characteristic calorimetric curves are shown in Fig. 2.

DSC analysis of samples from ingots 1 and 3 showed no peaks for either forward or reverse transformations within the temperature range studied. Ingot 2, however, showed a reverse *MT* with starting and finishing temperatures of $63\text{ }^\circ\text{C}$ and $124\text{ }^\circ\text{C}$, respectively. This wide temperature range is typical for as-cast ingots due to potential internal stresses and segregation.

To improve homogeneity, ingot 1 was initially subjected to a 12-hour homogenization annealing at $1,100\text{ }^\circ\text{C}$ in vacuum. However, the ingot melted during annealing, possibly due to the formation of phases with lower melting temperatures during cooling after melting. Therefore, it was decided not to

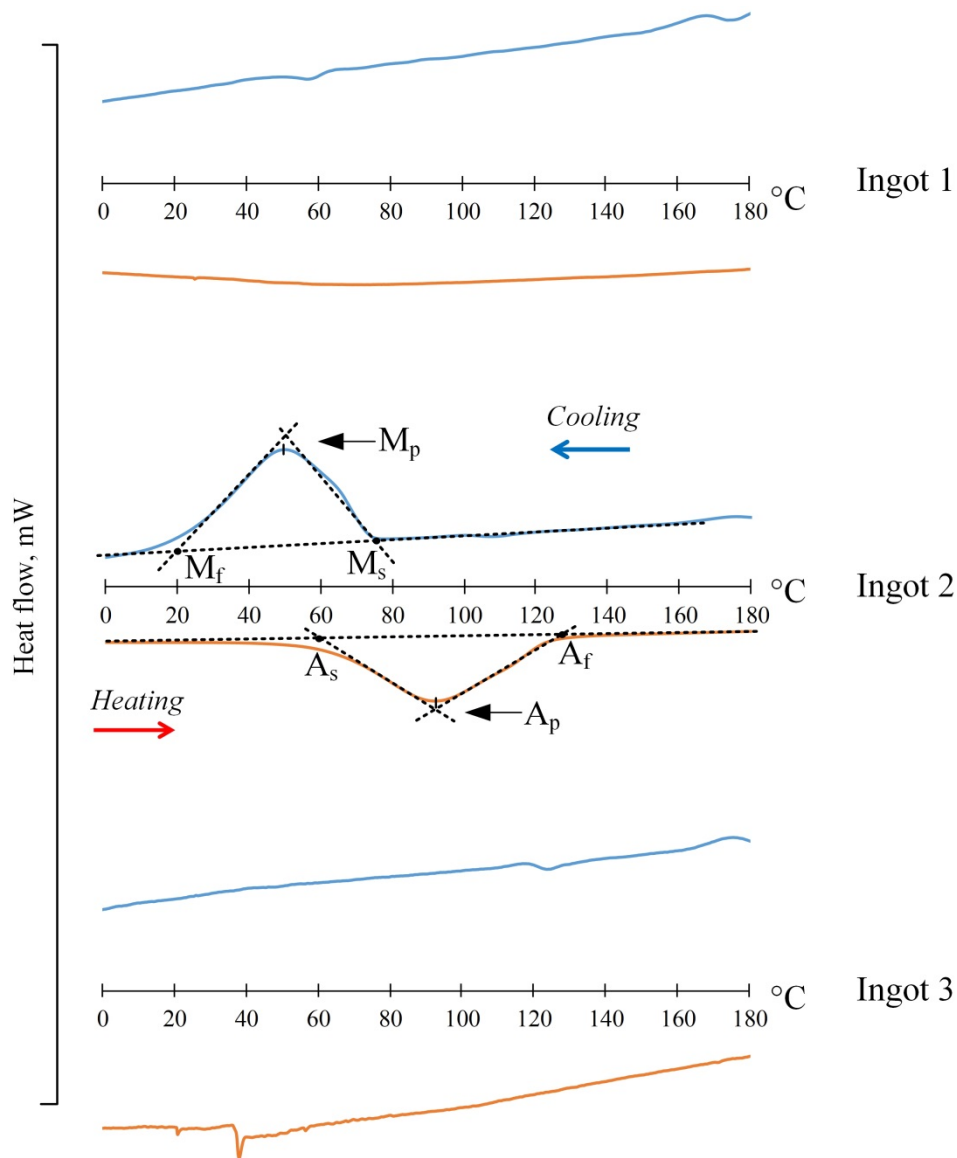


Fig. 2. Calorimetric curves of ingots 1, 2, and 3 of *TiNiHf SMA*

use homogenization annealing, and ingots 2 and 3 were deformed in the as-cast state. Homogenization annealing was therefore excluded from the production process for *TiNiHf SMA* semi-finished products to optimize the technology.

Production of TiNiHf SMA semi-finished products

Before deformation, the ingots were cut into two parts. The resulting ingots had the following dimensions: **2-1** – $10.4 \times 18.5 \times 53.1$ mm and **2-2** – $10.4 \times 18.5 \times 77.1$ mm; **3-1** – $9.8 \times 17.8 \times 52.1$ mm and **3-2** – $9.8 \times 17.8 \times 76.7$ mm.

Hot deformation of ingots **2-1** and **3-1** was first performed by longitudinal rolling at 850 °C. The samples were preheated for 15 minutes without a protective atmosphere to improve rolling workability, unlike previous studies [23] where heating was in a protective argon atmosphere, with 3–5 minute reheating before each pass. The relative strain in one pass was kept below 15%. Hot rolling of ingot **2-1** produced a sheet with dimensions $2.2 \times 27.5 \times 167.9$ mm. However, ingot **3-1** fractured after only 2 passes, accumulating a relative strain of 12%. Considering the lack of distinct peaks on the calorimetric curves, the melting of the similar ingot **1** during homogenization annealing, and the alloy's low workability, it's likely that ingot **3** contained many undesirable secondary phases formed during cooling after melting or during heating for rolling. This suggests that the alloy with 5 at.% *Hf* has better workability than the alloy with 10 at.% *Hf*. Fig. 3 shows photos of the sheet from ingot **2-1** and the fractured ingot **3-1**.



Fig. 3. Photographs of the obtained sheet from ingot **2-1** (*TiNiHf* alloy) with a thickness of 2.2 mm (a) and ingot **3-1** after fracture (b)

Further deformation by hot bar rolling (*HBR*) and rotary forging (*RF*) was only done on ingot **2-2** of the *TiNiHf* alloy with 5 at.% *Hf*. Initially, two passes were rolled in one caliber from a single heating cycle, taking advantage of deformation heating. However, when switching to the second caliber, cracks appeared at the back end of the ingot. This suggests that the alloy has a narrow temperature range for plastic deformation. To prevent the ingot from cooling down, it was reheated after each pass. Changing the rolling pattern and eliminating the second pass without preheating resulted in successful rolling without fracture or new cracks. This produced a rectangular bar measuring $6.9 \times 8.5 \times 236.4$ mm. After bar rolling, a 150 mm long sample was cut from the bar for rotary forging. Rotary forging was carried out at a deformation temperature of 850 °C, with a relative strain per pass below 10%, and the ingot was heated between each pass for 10-15 minutes. This produced a rod with a diameter of 119 mm.

It's worth noting that, unlike the approach in [23], the section of ingot **2** used here was rotary forged after prior deformation rather than in the as-cast state. This highlights the potential for combining hot bar rolling and rotary forging to produce *TiNiHf* SMA rods. Fig. 4 shows a photo of the bars after rolling and rotary forging.

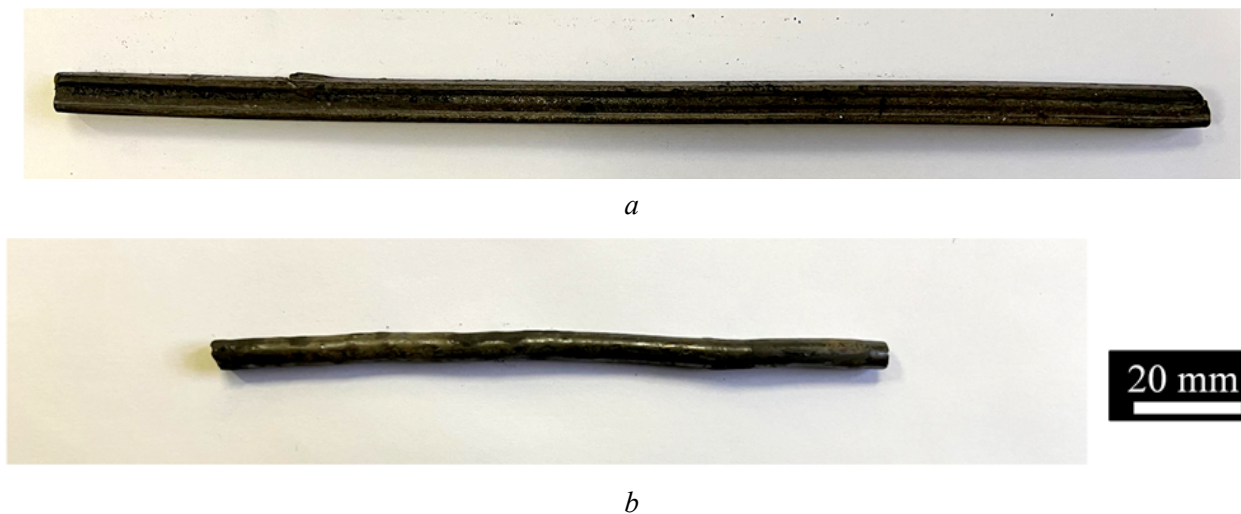


Fig. 4. Photograph of a *TiNiHf* alloy rod after caliber rolling (a) and rotary forging (b)

It should be noted that rotary forging had difficulties with rod alignment and chipping at the ends, likely due to cooling. Because of this, further rotary forging to smaller diameters (which would cool even faster) wasn't attempted.

Next, a $2.1 \times 27.5 \times 56$ mm sample was cut from the hot-rolled sheet from ingot **2-1** for cold rolling (*CR*). After cutting, the sample was cleaned to remove the surface oxide layer by grinding and chemical etching in a mixture of nitric and hydrofluoric acids. The sheet thickness before rolling was 2.1 mm. Cold rolling was carried out with a relative strain per pass below 10%. Prior work found the critical relative strain for cold rolling *TiNiHf* alloy to be 20% [22]. Therefore, cold rolling was carried out with intermediate annealing at a temperature of 850 °C for 10 minutes upon reaching a relative degree of deformation close to 20%. After cold rolling to 1.04 mm, a sample was cut from the sheet for further cold rolling to fracture to redetermine the critical strain. Fig. 5 shows the sheet before and after cold rolling, thus concluding our description of the cold rolling process.

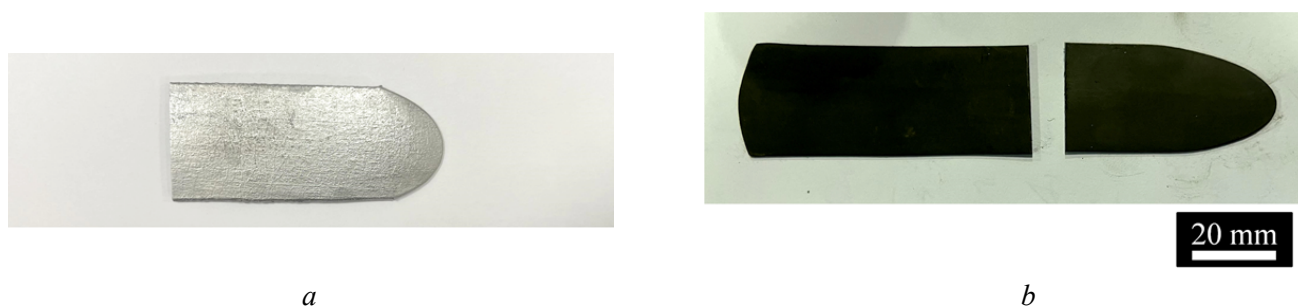


Fig. 5. General view of the *TiNiHf* SMA sheets before (a) and after (b) cold rolling

Cold rolling the *TiNiHf* SMA sample to its critical strain showed that fracture (a through-crack at the front end) occurred after a total relative strain of 23%, with a final sample thickness of 0.93 mm. This confirms that intermediate annealing is needed during cold rolling of *TiNiHf* alloy samples after a total strain of 20%.

Next, we studied how the phase composition and mechanical properties of the *TiNiHf* + 5 at.% *Hf* alloy changed depending on the processing method.

Investigation of the phase state and mechanical properties of *TiNiHf* SMA samples following application of various deformation methods

Fig. 6 shows the *Vickers* hardness of alloy 2 after deformation using different methods.

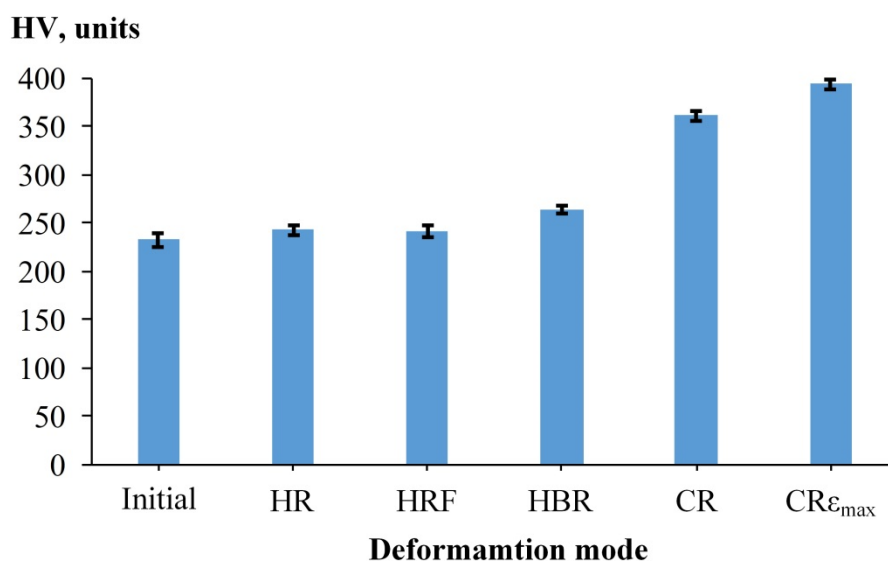


Fig. 6. Hardness of *TiNiHf* SMA samples after various deformation methods

Hot deformation slightly increased the *Vickers* hardness compared to the as-cast ingot 2 (232 HV): hardness after *HR* and *HRF* was about 242 HV, and after *HBR* it was 264 HV. This is typical for high-temperature heat treatment and related to dynamic and static recrystallization. Cold deformation to 1 mm thickness greatly increased hardness to 362 HV, with a maximum of 394 HV after *CR* to the critical strain leading to fracture. This is likely due to the increased crystal lattice defects after *CR*. The hot deformation results suggest that it occurs at a steady stage with dynamic recrystallization and stress relaxation from deformation hardening, unlike *CR*, which results in a heavily deformed structure.

Fig. 7 shows the X-ray analysis results for alloy 2 after various deformation methods.

X-ray analysis showed that martensite was the main phase in alloy 2 samples at room temperature, both before and after deformation. This agrees with the *DSC* data. The absence of *B2*-austenite peaks confirms that the reverse *MT* occurs above room temperature. $(Ti, Hf)_2Ni$ phase lines, formed during cooling after

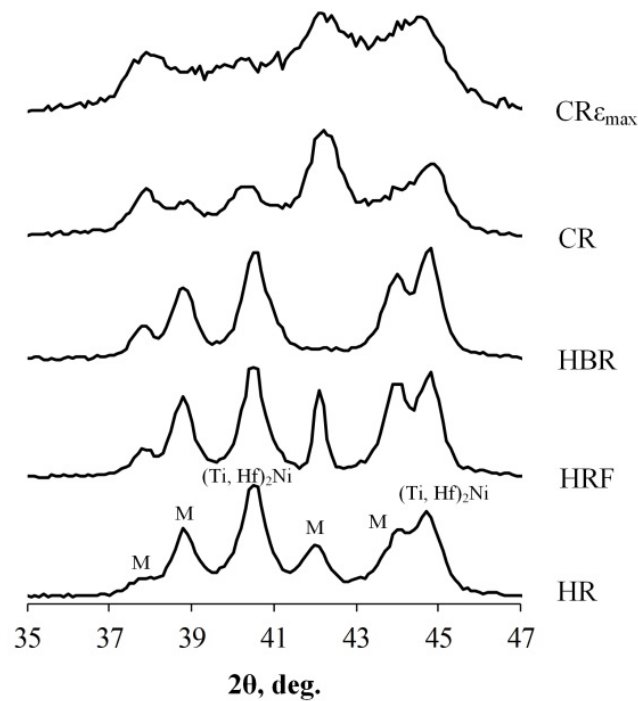


Fig. 7. X-ray diffraction patterns of *TiNiHf SMA* samples after the studied processing methods

melting, were seen at 2θ angles of 41° and 45° . Hot deformation didn't significantly broaden the X-ray lines, but cold rolling did. The changes in the sample line profile after cold rolling confirm significant deformation hardening and increased crystal structure defects.

Fig. 8 and Table 2 show the martensitic transformation temperature range (*TRMT*) measured by *DSC* after the different processing methods on ingot 2. Fig. 2 shows the initial *DSC* curves of the *TiNiHf SMA* ingots.

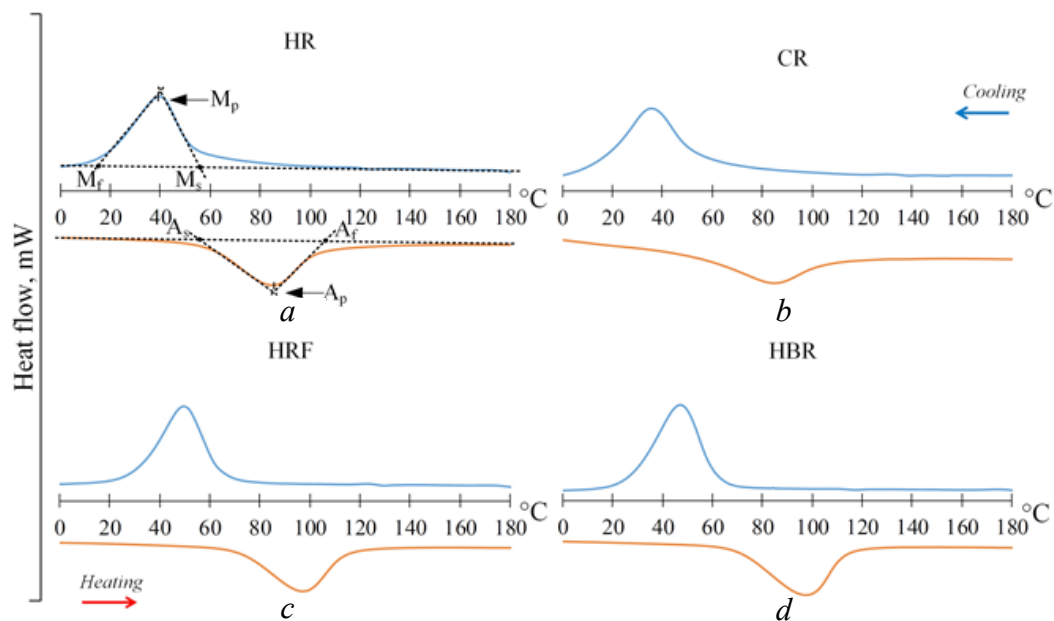


Fig. 8. Calorimetric curves of the samples of ingot 2 (*TiNiHf SMA*) after the studied processing methods: hot rolling (HR) (a), cold rolling (CR) (b), hot rotary forging (HRF) (c), and hot longitudinal rolling (HLRR) (d)

Table 2

Martensitic transformation temperatures of processed *TiNiHf SMA* (Ingot 2)

Sample	Direct transformation			Reverse transformation		
	$M_s, ^\circ\text{C}$	$M_p, ^\circ\text{C}$	$M_f, ^\circ\text{C}$	$A_s, ^\circ\text{C}$	$A_p, ^\circ\text{C}$	$A_f, ^\circ\text{C}$
Initial	74	50	21	62	92	124
<i>HR</i>	54	40	17	61	85	105
<i>HRF</i>	65	50	31	71	97	115
<i>HBR</i>	62	47	27	70	97	113
<i>CR</i>	54	36	17	52	85	107

The results show that neither hot nor cold deformation significantly changes the martensitic transformation temperatures; they remain relatively stable with fluctuations under 10 °C. However, there's a trend of decreasing forward MT (A_p) temperature compared to the as-cast state of ingot 2. Even so, this temperature stays above 105 °C in all cases, indicating that the *TiNiHf* alloy maintains its high-temperature shape memory behavior.

Conclusion

A comprehensive investigation was undertaken to assess the feasibility of producing a range of semi-finished products from *TiNiHf* shape memory alloys containing 5 and 10 at.% *Hf* with reduced *Ni* content, utilizing various deformation methods. Based on the findings of this study, the following conclusions can be drawn:

The *TiNiHfSMA* with 10 at.% *Hf* lacks sufficient technological plasticity for thermomechanical treatment by the considered deformation methods.

The *TiNiHf SMA* with 5 at.% *Hf* has sufficient technological plasticity. Various deformation methods were applied to the alloy (hot and cold longitudinal rolling, bar rolling, rotary forging). High-quality semi-finished products in the form of sheets and rods of various sizes were obtained.

Hot deformation increases hardness from 232 HV (as-cast) to 242 HV (*HR/HRF*) and 264 HV (*HBR*). Cold deformation significantly increases hardness, reaching 362 HV (1 mm thick sheet) and 394 HV (rolling to critical strain).

The characteristic temperatures of the forward and reverse martensitic transformations in the *TiNiHfSMA* with 5 at.% *Hf* remain stable after deformation. Deformation slightly decreases the finishing temperature of the reverse martensitic transformation (A_p) (to 19 °C) compared to the as-cast ingot. However, A_f remains above 105 °C, confirming their high-temperature shape memory behavior.

Thermomechanical processing using hot and cold rolling and rotary forging is a promising method for producing *TiNiHf SMA* semi-finished products with 5 at.% *Hf* and improving the alloy's functional and mechanical properties after melting.

References

1. Sadashiva M., Sheikh M.Y., Khan N., Kurbet R., Gowda T.D. A review on application of shape memory alloys. *International Journal of Recent Technology and Engineering (IJRTE)*, 2021, vol. 9 (6), pp. 111–120. DOI: 10.35940/ijrte.F5438.039621.
2. Nair V.S., Nachimuthu R. The role of NiTi shape memory alloys in quality of life improvement through medical advancements: A comprehensive review. *Proceedings of the Institution of Mechanical Engineers, Part H: Journal of Engineering in Medicine*, 2022, vol. 236 (7), pp. 923–950. DOI: 10.1177/09544119221093460.
3. Kim M.S., Heo J.K., Rodrigue H., Lee H.T., Pané S., Han M.W., Ahn S.H. Shape memory alloy (SMA) actuators: The role of material, form, and scaling effects. *Advanced Materials*, 2023, vol. 35 (33), p. 2208517. DOI: 10.1002/adma.202208517.



4. Khmelevskaya I., Komarov V., Kawalla R., Prokoshkin S., Korpala G. Features of Ti-Ni alloy structure formation under multi-axial quasi-continuous deformation and post-deformation annealing. *Materials Today: Proceedings*, 2017, vol. 4 (3), pp. 4830–4835. DOI: 10.1016/j.matpr.2017.04.079.
5. Karelin R., Komarov V., Khmelevskaya I., Cherkasov V., Andreev V., Yusupov V., Prokoshkin S. Effect of temperature-deformation regimes of equal channel angular pressing in core-shell mode on the structure and properties of near-equiatomic titanium nickelide shape memory alloy. *Journal of Alloys and Compounds*, 2024, vol. 1005, p. 176071. DOI: 10.1016/j.jallcom.2024.176071.
6. Komarov V., Karelin R., Khmelevskaya I., Yusupov V., Gunderov D. Effect of post-deformation annealing on structure and properties of nickel-enriched Ti-Ni shape memory alloy deformed in various initially deformation-induced structure states. *Crystals*, 2022, vol. 12 (4), p. 506. DOI: 10.3390/cryst12040506.
7. Karelin R., Komarov V., Khmelevskaya I., Andreev V., Yusupov V., Prokoshkin S. Structure and properties of TiNi shape memory alloy after low-temperature ECAP in shells. *Materials Science and Engineering: A*, 2023, vol. 872, p. 144960. DOI: 10.1016/j.msea.2023.144960.
8. Parida J., Mishra S.C. NiTi-based ternary alloys. *Nickel-Titanium Smart Hybrid Materials*. Elsevier, 2022, pp. 191–213. DOI: 10.1016/B978-0-323-91173-3.00020-1.
9. Parvizi S., Hashemi S.M., Moein S. NiTi shape memory alloys: properties. *Nickel-titanium smart hybrid materials*. Elsevier, 2022, pp. 399–426. DOI: 10.1016/B978-0-323-91173-3.00021-3.
10. Ahmad M. Effect of ternary element addition on properties of TiNi-based shape memory alloys for engineering and medical applications. *Journal of Metastable and Nanocrystalline Materials*, 2023, vol. 36, pp. 7–20. DOI: 10.1016/B978-0-323-91173-3.00021-3.
11. Sampath S., Nguyen T.A. NiTi-based ternary shape-memory alloys. *Nickel-titanium smart hybrid materials*. Elsevier, 2022, pp. 123–137. DOI: 10.1016/B978-0-323-91173-3.00006-7.
12. Tong Y., Shuitcev A., Zheng Y. Recent development of TiNi-based shape memory alloys with high cycle stability and high transformation temperature. *Advanced Engineering Materials*, 2020, vol. 22, p. 1900496. DOI: 10.1002/adem.201900496.
13. Karakoc O., Atli K.C., Evirgen A., Pons J., Santamarta R., Benafan O., Noebe R.D., Karaman I. Effects of training on the thermomechanical behavior of NiTiHf and NiTiZr high temperature shape memory alloys. *Materials Science and Engineering: A*, 2020, vol. 794, p. 139857. DOI: 10.1016/j.msea.2020.139857.
14. Tagiltsev A.I., Panchenko E.Y., Timofeeva E.E., Chumlyakov Y.I., Fatkullin I.D., Marchenko E.S., Karaman I. The effect of stress-induced martensite aging in tension and compression on B2-B19' martensitic transformation in $\text{Ni}_{50.3}\text{Ti}_{32.2}\text{Hf}_{17.5}$ high-temperature shape memory alloy. *Smart Materials and Structures*, 2021, vol. 30 (2), p. 025039. DOI: 10.1088/1361-665X/abdaa8.
15. Shuitcev A., Gunderov D.V., Sun B., Li L., Valiev R.Z., Tong Y.X. Nanostructured $\text{Ti}_{29.7}\text{Ni}_{50.3}\text{Hf}_{20}$ high temperature shape memory alloy processed by high-pressure torsion. *Journal of Materials Science & Technology*, 2020, vol. 52, pp. 218–225. DOI: 10.1016/j.jmst.2020.01.065.
16. Akgul O., Tugrul H.O., Kockar B. Effect of the cooling rate on the thermal and thermomechanical behavior of NiTiHf high-temperature shape memory alloy. *Journal of Materials Research*, 2020, vol. 35, iss. 12, pp. 1572–1581. DOI: 10.1557/jmr.2020.139.
17. Shuitcev A., Vasin R.N., Balagurov A.M., Li L., Bobrikov I.A., Tong Y.X. Thermal expansion of martensite in $\text{Ti}_{29.7}\text{Ni}_{50.3}\text{Hf}_{20}$ shape memory alloy. *Intermetallics*, 2020, vol. 125, p. 106889. DOI: 10.1016/j.intermet.2020.106889.
18. Catal A.A., Bedir E., Yilmaz R., Canadinc D. Design of a NiTiHf shape memory alloy with an austenite finish temperature beyond 400 °C utilizing artificial intelligence. *Journal of Alloys and Compounds*, 2022, vol. 904, p. 164135. DOI: 10.1016/j.jallcom.2022.164135.
19. Kim J.H., Park C.H., Kim S.W., Hong J.K., Oh C.X., Jeon Y.M., Kim K.K., Yeom J.T. Effects of microstructure and deformation conditions on the hot formability of Ni-Ti-Hf shape memory alloys. *Journal of Nanoscience and Nanotechnology*, 2014, vol. 14, pp. 9548–9553. DOI: 10.1166/jnn.2014.10191.
20. Babacan N., Bilal M., Hayrettin C., Liu J., Benafan O., Karaman I. Effects of cold and warm rolling on the shape memory response of $\text{Ni}_{50}\text{Ti}_{30}\text{Hf}_{20}$ high-temperature shape memory alloy. *Acta Materialia*, 2018, vol. 157, pp. 228–244. DOI: 10.1016/j.actamat.2018.07.009.
21. Benafan O., Bigelow G.S., Garg A., Noebe R.D., Gaydos D.J., Rogers R.B. Processing and scalability of NiTiHf high-temperature shape memory alloys. *Shape Memory and Superelasticity*, 2021, vol. 7, pp. 109–165. DOI: 10.1007/s40830-020-00306-x.
22. Stolyarov V.V., Andreev V.A., Karelin R.D., Ugurchiev U.Kh., Cherkasov V.V., Komarov V.S., Yusupov V.S. Deformability of TiNiHf shape memory alloy under rolling with pulsed current. *Obrabotka metallov*



(*tekhnologiya, oborudovanie, instrumenty*) = *Metal Working and Material Science*, 2022, vol. 24, no. 3, pp. 66–75. DOI: 10.17212/1994-6309-2022-24.3-66-75.

23. Karelin R., Komarov V., Cherkasov V., Yusupov V., Prokoshkin S., Andreev V. Production mechanical and functional properties of long-length TiNiHf rods with high-temperature shape memory effect. *Materials*, 2023, vol. 16 (2), p. 615. DOI: 10.3390/ma16020615.

24. Keret-Klainer M., Padan R., Khoptiar Y., Kauffmann Y., Amouyal Y. Tailoring thermal and electrical conductivities of a Ni-Ti-Hf-based shape memory alloy by microstructure design. *Journal of Materials Science*, 2022, vol. 57, iss. 25, pp. 12107–12124. DOI: 10.1007/s10853-022-07383-6.

Conflicts of Interest

The authors declare no conflict of interest.

© 2025 The Authors. Published by Novosibirsk State Technical University. This is an open access article under the CC BY license (<http://creativecommons.org/licenses/by/4.0>).